Effect of Ni Charge States on Structural, Electronic, Magnetic, and Optical Properties of InN

ARTICLE *in* THE JOURNAL OF PHYSICAL CHEMISTRY A · JUNE 2013

Impact Factor: 2.69 · DOI: 10.1021/jp402876f · Source: PubMed

5 AUTHORS, INCLUDING:

Zahid Usman
University of Lahore
40 PUBLICATIONS **169** CITATIONS
SEE PROFILE

Chiuanbao Cao
Beijing Institute of Technology
274 PUBLICATIONS **3,397** CITATIONS
SEE PROFILE

Matiullah Khan
Kohat University of Science and Technology
44 PUBLICATIONS **164** CITATIONS
SEE PROFILE

Abdul Rehman Khan Niazi
Beijing Institute of Technology
4 PUBLICATIONS **8** CITATIONS
SEE PROFILE

THE JOURNAL OF PHYSICAL CHEMISTRY A

Article

pubs.acs.org/JPCA

Effect of Ni Charge States on Structural, Electronic, Magnetic, and Optical Properties of InN

Zahid Usman,[†] Chuanbao Cao,*[,†] Matiullah Khan,[‡] Tariq Mahmood,[†] and A. R. Niazi[†]

[†]Research Centre of Materials Science, School of Material Science and Engineering, Beijing Institute of Technology, Beijing 100081, China

[‡]Department of Inorganic Nonmetallic Materials, School of Materials Science and Engineering, University of Science and Technology, Beijing 100083, China

ABSTRACT: The first-principles study of Ni-doped InN has been carried out to explore the doping effect of various charge states of Ni on the structural, electronic, magnetic, and optical properties of InN using generalized gradient approximation. Structural properties like lattice parameters, aspect ratios, bond lengths, and formation energies of (In, Ni) N are used to determine the stability of each doped system. The formation energies of (In, Ni)N systems decrease with the increase in charge state of nickel, while the bond lengths show an opposite trend. The DOS diagram shows that the introduction of Ni-d states within the bang gap region reduces the band gap for Ni^{1+}- and Ni^{2+}-doped InN, while the isolated states are generated in the case of Ni^{3+}- and Ni^{4+}-doped systems. The Ni^{1+}-, Ni^{3+}-, and Ni^{4+}-doped InN systems are ferromagnetic in nature, whereas the (In, Ni^{2+})N depicts spin-glass-like behavior. The best possible magnetization is obtained for (In, Ni^{4+})N with a total magnet moment of 2.42 μ_B per supercell. Because of the presence of nickel impurities, the optical properties of InN have been significantly improved. The pure and Ni^{3+}- and Ni^{4+}-doped InN systems show nearly the same values of absorption edges (~0.56 eV), in contrast with the Ni^{1+}- and Ni^{2+}-doped systems, where these values are 0.37 and 0.51 eV, respectively. The shift in absorption edges of Ni^{1+}- and Ni^{2+}-doped InN to lower energies and increase in the intensity of absorption and broadening of absorption peaks can be attributed to the pronounced band-gap reduction for these systems. A negligible shift of absorption edges in the case of Ni^{3+}- and Ni^{4+}- doped InN is the characteristic of isolated charge states introduced around the Fermi level, which inhibit the band gap reduction, and hence the optical properties are not improved as expected. This study demonstrates an important fact that for best possible optical device applications Ni^{1+}-doped InN system is excellent, while for better magnetic properties the (In, Ni^{4+})N is more suitable.

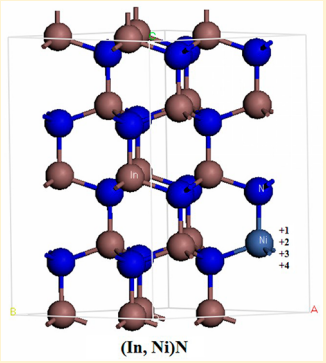

1. INTRODUCTION

The discovery of dilute magnetic semiconductors (DMSs) has initiated immense interest due to their vital applications in relatively new and revolutionary field of study named as spin-electronics, considering both the spin and charge of the electron simultaneously. The field of spintronics has the potential to improve the speed as well as the storage capacity of microelectronic devices.[1] It is suggested by Furdyna[2] that the exchange interactions among the d electrons of transition metals and s and p electrons of host material are responsible for the optoelectronic and magnetic properties of DMS. The room-temperature ferromagnetism in GaN[3−6] and ZnO[7,8] has further infused new spirit in the field of DMS materials.

Except group III−V nitrides (InN, AlN, GaN), another class of DMS nitride materials such as PtN, PdN has been introduced by Eyert et al.[9] These materials have shown excellent ferromagnetic properties when doped with manganese (Mn) and iron (Fe). Similarly, scandium nitride (ScN) doped with Mn[10] has exhibited excellent magnetic properties, too.

InN is a narrow bang gap semiconductor mostly used in solar cells, laser diodes, transistors, and light-emitting diodes. Surprisingly, the InN enjoys high carrier drift velocity,[11] Hall mobility,[12] and tunability of band gap up to 2 eV through gallium alloying.[13] The most striking feature of InN is its weak spin−orbit coupling (0.003 eV),[14] which is a primary condition for long spin diffusion length and time. These factors comprehensively reduce the spin−orbit scattering and the spin relaxation rates in turn. These features are more than enough to declare its suitability in spintronic applications. Cr- and Mn-doped InN thin films are synthesized successfully by Ney et. al,[15] which have shown ferromagnetic properties.

The first-principles surface studies of InN have been performed previously by many authors,[16−19] but no attempts are made to explore its electronic, magnetic, and optical properties in bulk form. It is a well-established fact that the defects and impurities are a major route to alter the band structure and hence the electronic and optical properties of semiconductors. Additionally, less attention has been paid to investigating the effect of different charge states of dopant on the above-mentioned properties.

Keeping in mind the possible charge states of nickel (Ni^{1+}, Ni^{2+}, Ni^{3+}, and Ni^{4+}), a systematic first-principles study of the

Received: March 24, 2013
Revised: June 14, 2013
Published: June 17, 2013

structural, electronic, magnetic, and optical properties of Ni-doped InN with above-mentioned charge states has been carried out for the first time. The stability of different charge states is discussed in the context of formation energies, lattice parameters, bond lengths, and aspect ratios (c/a). We have observed that Ni^{1+}-doped InN system is excellent for optical properties, while the (In, Ni^{4+})N is more suitable for better magnetic properties.

2. COMPUTATIONAL DETAILS

Spin-polarized density functional theory via CASTEP code is implemented to explore the structural, magnetic, electronic, and optical properties of Ni-doped wurtzite InN at cation site. The electron−electron exchange interactions deal with generalized gradient approximation suggested by Perdew−Burke−Ernzerhof (GGA-PBE),[20] whereas the electron ion exchange interactions cope with ultrasoft pseudopotential method.[21] The electronic wave functions are expanded in plane-wave basis set with a cut off energy of 380 eV, and the Brillouin zone integration is carried out using Monkhorst-Pack grid of 3 × 3 × 3 k points. The atoms are allowed to relaxed until the force on each atom and the total energy convergence are set to be 0.05 eV/Å and 2.0 × 10^{-5} eV/atom. We have considered a 32-atom InN supercell, where the different charge states (Ni^{1+}, Ni^{2+}, Ni^{3+}, and Ni^{4+}) are assigned to the nickel, substituted at In sites individually. The effect of various charge states of Ni on structural, electronic, magnetic, and optical properties of pure InN has been discussed in detail.

3. RESULTS AND DISCUSSION

Considering different charge states of nickel, we have geometrically optimized the Ni-doped InN supercells, and different structural parameters like the equilibrium lattice parameters and ground-state energies are predicted. The Ni^{1+}-doped InN manifests the lattice parameters a = 3.502 Å and c = 5.643 Å, slightly underestimated with respect to their experimental counterparts, whose values are 3.540 and 5.706 Å,[22] respectively. The c/a ratio in this case is 1.6112, which shows good consistency with the experimental value of 1.6120,[22] as shown in Table 1. Because the ionic radii of Ni^{1+} as compared with In ion is significantly smaller, the resultant equilibrium lattice parameters are reduced as compared with the experimental values, and thus substituting Ni instead of In leads to a shrinkage of supercell. Because of the shrinkage of Ni^{1+}-doped InN supercell, the nitrogen atoms are attracted toward Ni atom, and hence the In−N bond length (1.87 Å) is reduced corresponding to the experimental value of 2.15 Å.[23] The calculated bond lengths between Ni−N for various charge states of Ni-doped InN are calculated and shown in Figure 1.

Table 1. Various Physical Quantities for Ni-Doped InN

(In, Ni^{1+})N	(In, Ni^{2+})N	(In, Ni^{3+})N	(In, Ni^{4+})N	InN experiment
3.5025	3.544	3.585	3.63	3.540[22]
5.643	5.70	5.80	5.86	5.706[22]
1.6112	1.608	1.618	1.612	1.6120[22]
1.87	1.9	1.97	2.10	
2.12	2.18	2.19	2.22	2.15[23]
5.8	−6.5	−15.5	−22.5	
0.98		1.0021	2.42775	
0.37	0.51	0.56	0.56	

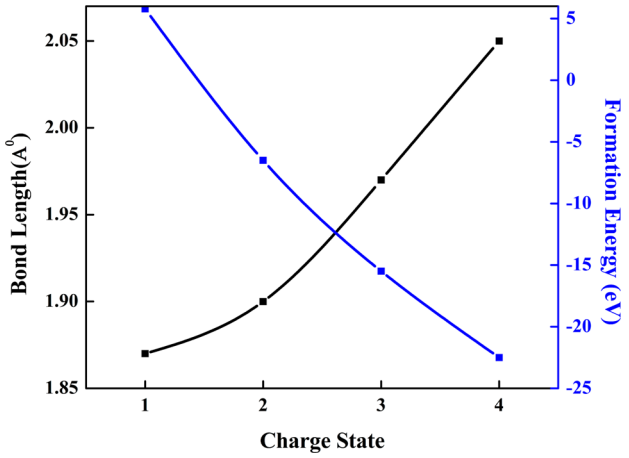

Figure 1. Bond length (Å) between Ni−N atoms and formation energies (eV) plotted against various nickel charge states.

For Ni-doped InN, Ni−N bond lengths increase with the increase in nickel charge states. Figure 1 shows that the bond length between Ni−N atoms in the case of (In, Ni^{4+})N is 2.10 Å, very close to the experimental bond length between In−N (2.20 Å) in pure InN[23] measured through EXAFS analysis. (In, Ni^{4+})N has c/a value exactly the same as experiment (1.612),[21] confirming an important fact that doping of Ni^{4+} produces the least distortion within the InN structure. To address the stability issue of Ni dopant in InN, we have computed the formation energies as shown in Table 1, relative to the different charge states of Ni-doped InN[5] using the following formula:

$$E_{form} = E_s + n(E_{In} - E_{Ni}) - E_b$$

where E_{form}, E_s, E_{In}, E_{Ni}, and E_b belong to the formation energy, total energy of Ni-doped supercell with n indium atoms replaced by Ni atoms, energy of isolated indium atom, isolated Ni atom's energy, and total energy of bulk InN supercell in pure form, respectively. The formation energies calculated through above formula are shown in Figure.1. The formation energy in case of Ni^{1+}doped InN is 5.8 eV. From Figure.1, it is clear that, the formation energy decreases with increasing nickel charge state, and obtains its lowest value of −22.59 eV for Ni^{4+} doped InN. Gradual decrease in formation energy with respect to the increase in charge states infers that the effect of increase in nickel charge state is actually stabilizing the Ni doped InN systems, while the structural parameters are shifting toward pure InN at the same time.

To elucidate the effect of doping and further explore the origin of ferromagnetism in Ni-doped InN, we have presented a thorough picture of DOS diagram. The total and N-p DOS for pure and extrinsic InN are shown in Figure 2a, whereas the d-DOS for various charge states of Ni-doped InN are shown in Figure 2b. The total and N-p DOS for pure InN reveal that the valence band, whose width is 5.7 eV, is heavily populated with N-p states.

The total DOS for pure InN (Figure 2a) shows that the band gap for pure InN is 0.72, which is very close to the experimental value of 0.7 eV.[24] The DOS diagram shows that substitution of In with Ni creates Ni-d DOS around the Fermi level, and valence band of InN is modified extensively when the charge state of impurity atom increases. From Figure 2b, the inclusion of Ni-d DOS reduces the band gap in the case of Ni^{1+}- and Ni^{2+}-doped InN systems. Isolated charge states appear within the band gap region for Ni^{3+}- and Ni^{4+}-doped InN systems, as

dx.doi.org/10.1021/jp402876f | J. Phys. Chem. A 2013, 117, 5650−5654

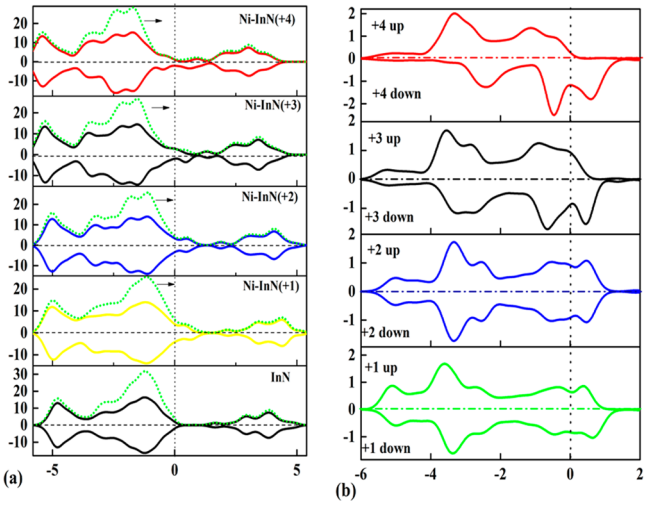

Figure 2. (a) Total and N-p DOS for Pure and (In, Ni)N systems and (b) Ni-d DOS for doped InN.

shown in Figure 2b. The presence of these charge states may reduce the optical absorption of the respective doped systems later on. The doping of InN with different charge states of nickel clearly modifies the conduction band of Ni-doped InN as compared with pure InN, where the Ni-d states also appear in minimum conduction band region.

When Ni is incorporated in InN, the d states of Ni divide into d_{xy}, d_{xz}, d_{yz}, d_{z^2}, and $d_{x^2-y^2}$ states due to crystal field splitting. For substitutional doping, Ni-d states (d_{xy}, d_{xz}, d_{yz},) strongly hybridize with host p states and form bonding (t_b) and antibonding states (t_a), whereas the Ni d_{z^2} and $d_{x^2-y^2}$ states reside at the Fermi level, forming nonbonding states (t_e states). At valence band maximum (VBM), the Ni d orbitals lie above the host N p orbitals, which is why clear energy bands are formed inside the band gap. Figure 2a shows that N-p states are moving to the right in all Ni-doped InN systems as compared with the pure one, although Ni-d states are moving to the left due to the p-d repulsion. The (In, Ni)N may not be suitable for spintronic applications because the spin-polarization at the Fermi level is not 100% and attains its highest value for Ni^{4+}-doped InN unlike the other half-metallic systems, as suggested by Sato et al.[25] The careful analysis of d-DOS reveals that the Ni^{1+}-, Ni^{3+}-, and Ni^{4+}-doped InN systems are ferromagnetic in nature and the magnetic moments related to these charge states are 0.98, 1.0021, and 2.42775 μ_B, respectively, as summarized in Table 1, but for Ni^{2+}-doped InN, the spin polarization is zero; therefore, the state is predicted to be spin-glass state. The increase in magnetic moment from Ni^{3+}- to Ni^{4+}-doped InN may belong to the exchange of charge between majority d states (t_b) and minority t_e states.

To get an idea about the possible application of Ni-doped InN in optoelectronic devices, we have further investigated its effect on the optical properties of InN. The optical properties include the dielectric function, absorption spectrum, reflectivity, refractive index, and energy loss function. Subjected to the specific transition rules, the optical transitions occur between valence band and conduction band as a result of photon electric field. The imaginary part of dielectric function (ε_2), calculated from momentum matrix elements, is dependent on the frequency and is used to calculate all other optical quantities.

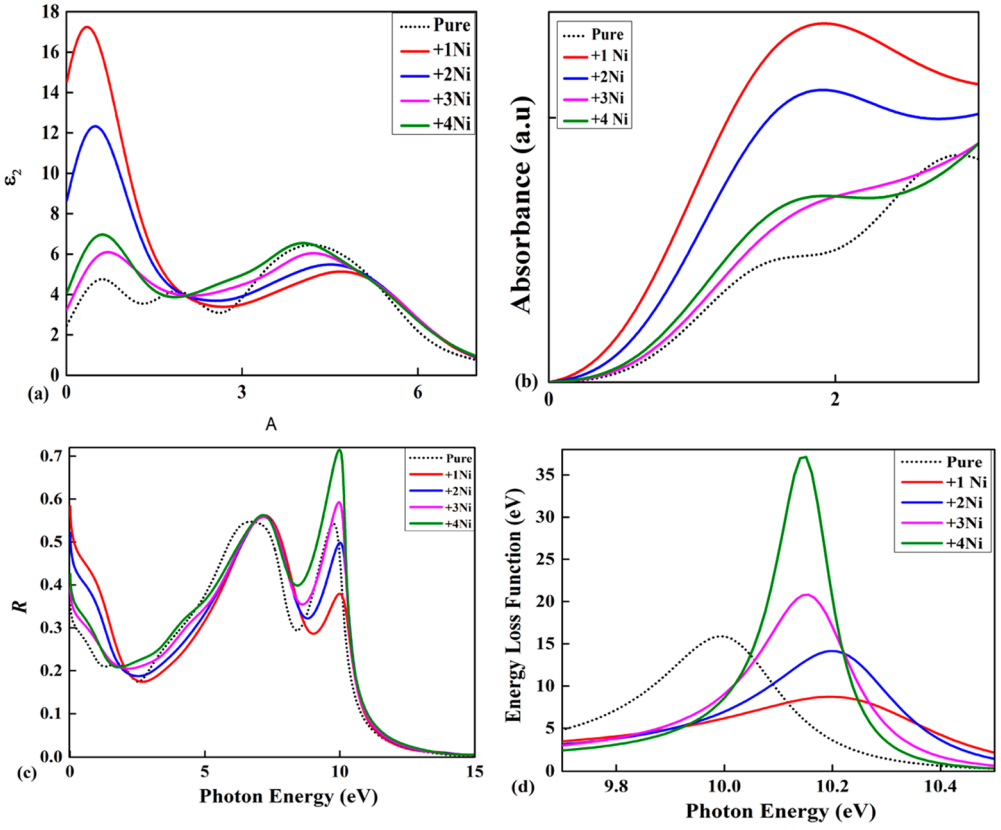

Figure 3. (a) Shows the imaginary part of dielectric function, (b) the absorption spectra, (c) reflectivity, and (d) energy loss function for pure and (In, Ni)N systems, respectively.

dx.doi.org/10.1021/jp402876f | J. Phys. Chem. A 2013, 117, 5650−5654

The comparative study of the optical properties of pure and doped InN with various charge states of nickel is presented in Figure 3. The imaginary part of dielectric function (Figure 3a) for intrinsic InN starts with a magnitude of 2.5 eV and increases with photon energy, depicting three peaks at 0.58, 1.8, and 4 eV relative to the transition from N-2p states at the top of valence band to the In-5s states at the lowest conduction band, In-3d and N-2p and In-3d to N-2s, respectively. The major peaks of dielectric function for InN doped with various charge states of Ni are broadened and shift toward lower energies. This shift of peaks is more obvious in the case of Ni^{1+}- and Ni^{2+}- doped InN systems. This shifting of peaks may arise due to the transfer of electrons from N-2p states in maximum valence band region to In-4s states.

Figure 3b presents a comparative description of the absorption spectra between the pure and doped InN systems. Here we can see that the effect of doping InN with nickel clearly modifies the absorption spectra as compared with pure InN. The absorption edges for pure and Ni^{3+}- and Ni^{4+}-doped InN exhibit nearly same value of 0.56 eV, as compared with those with Ni^{1+}- and Ni^{2+}-doped systems, which are 0.37 and 0.51 eV, respectively. The shifting of absorption edges to lower energies, overall increase in absorption intensity, and broadening of absorption peaks in the case of Ni^{1+}- and Ni^{2+}-doped systems can be ascribed to the considerable band gap reduction, as evident from Figure 2a, whereas the (In, Ni^{3+})N and (In, Ni^{4+})N systems encounter the presence of isolated charge states, which neither increase absorption nor play an extensive role in narrowing of band gap, as confirmed by TDOS plot in Figure 2a. Thus the shift of absorption edges toward lower energies is negligible and hence the intensity of absorption is also not increased as in former cases. The magnitude of absorption for (In, Ni^{1+})N is highest, which shows that this system is more suitable for optical device applications. Ni-doped InN with different charge states reveals an enhanced magnitude of reflectivity, pointing out a prominent band-gap reduction. The reflectivity of pure and doped systems decreases sharply after 10 eV, as shown in Figure 3c. The energy loss function for intrinsic InN is typically related to the plasma oscillations ($\omega_p = 4\pi ne^2/m_e$, where n is conduction electron density and m_e is the effective mass of conduction electrons) and increases with photon energy by obtaining its maximum value at ~10 eV. This should be kept in mind that for semiconductors the energy loss function corresponds to a situation where the electrons are no more bound to their respective lattice sites. Its maximum value corresponds to a point where the dielectric function is lowest, as apparent from Figure 3d. Because the dielectric functions for all doped systems are extinct at higher energies than intrinsic InN, the energy loss function is also shifted to the higher energies. The magnitude of maximum loss functions varies upon doping because it is dependent on conduction electron density and their effective masses. For Ni^{4+}-doped InN, the magnitude of energy loss function is maximum because of the effect of isolated charge states, which capture more electrons excited from the valence band when light is incident upon it.

4. CONCLUSIONS

Ni-doped InN have shown many interesting properties relative to the doping of various charge states of nickel impurity atom. The bond length of Ni−N increases with increasing nickel's charge states, while the formation energies drop conversely. The evaluation of structural parameters suggests that the Ni^{4+}-doped InN is the most stable doped system as compared with the pure InN. The doping of Ni in InN introduces d states around the Fermi level, where a pronounced band-gap reduction is found for Ni^{1+}- and Ni^{2+}-doped InN systems, while isolated charge states appear within the band gap region for Ni^{3+}- and Ni^{4+}-doped InN. The presence of these charge states may reduce the optical absorption of the respective doped systems later on. The Ni^{1+}-, Ni^{3+}-, and Ni^{4+}-doped InN systems are ferromagnetic in nature, whereas the (In, Ni^{2+})N depicts spin-glass-like behavior. The best possible magnetization is obtained for (In, Ni^{4+})N supercell, where the total magnet moment for 32 atom supercell is 2.42 μ_B. The optical properties of InN have been improved significantly with the doping of Ni as compared with the pure InN. The absorption edges for pure (In, Ni^{3+})N and (In,Ni^{4+})N are nearly the same, while those for (In, Ni^{1+})N and (In,Ni^{2+})N are shifted sufficiently to lower energies. This shift of absorption edges is due to the band-gap reduction. Furthermore, we have analyzed the imaginary part of dielectric function, reflectivity, and energy-loss function for pure and doped InN systems. This study demonstrates that the (In, Ni^{1+})N system is best for optical device applications, whereas the (In,Ni^{4+})N system shows excellent magnetic properties

AUTHOR INFORMATION

Corresponding Author

*E-mail: cbcao@bit.edu.cn. Tel: 0086-10-68913792.

Notes

The authors declare no competing financial interest.

ACKNOWLEDGMENTS

This work was supported by National Natural Science Foundation of China (20471007, 50972017) and the Research Fund for the Doctoral Program of Higher Education of China (20101101110026).

REFERENCES

(1) Dietal, T.; Ohno, H.; Matsukura, F.; Cibert, J.; Ferrand, D. Zener Model Description of Ferromagnetism in Zinc-Blende Magnetic Semiconductors. *Science* **2000**, *287*, 1019−1022.

(2) Furdyna, J. K. Diluted Magnetic Semiconductors. *J. Appl. Phys.* **1988**, *64*, 29−64.

(3) Park, S. E.; Lee, H. J.; Cho, Y. C.; Jeong, S. Y.; Cho, C. R.; Cho, S. Room Temperature Ferromagnetism in Cr-doped GaN Single Crystals. *Appl. Phys. Lett.* **2002**, *80*, 4187−4189.

(4) Munawar Basha, S.; Ramasubramanian, S.; Rajagopalan, M.; Kumar, J.; Won Kang, T.; Ganapathi Subramaniam, N.; Kwon, Y. Investigations on Cobalt Doped GaN for Spintronic Applications. *J. Cryst. Growth.* **2011**, *318*, 432−435.

(5) Munawar Basha, S.; Ramasubramanian, S.; Thangavel, R.; Rajagopalan, M.; Kumar, J. Magnetic Properties of Ni Doped Gallium Nitride with Vacancy Induced Defect. *J. Magn. Magn. Mater.* **2010**, *322*, 238−241.

(6) Pan, H.; Gu, B.; Eres, G.; Zhang, Z. Ab-Initio Study on Non-Compensated CrO Codoping of GaN for Enhanced Solar Energy Conversion. *J. Chem. Phys.* **2010**, *132*, 104501−104504.

(7) Zhi-Kuo, T.; Rong, Z.; Xu-Gao, C.; Qian, X.; Guo-Yu, Z.; Zi-Li, X.; Shu-Lin, G.; Yi, S.; You-Dou, Z. Optical and Magnetic Properties of Fe-Doped GaN Diluted Magnetic Semiconductors Prepared by MOCVD Method. *Chin. Phys. Lett.* **2008**, *25*, 1476−1478.

(8) Dietl, T. Ferromagnetic Semiconductors. *Semicond. Sci. Technol.* **2002**, *17*, 377−392.

(9) Houri, A.; Matar, S. F.; Eyert, V. Semi-Conducting (Half-Metallic) Ferromagnetism in Mn(Fe) Substituted Pt and Pd Nitrides. *Phys. Rev. B* **2010**, *82*, 241201−241205.

(10) Houri, A.; Matar, S. F.; Belkhir, M. A. Stability and Magnetic Properties of Mn-Substituted ScN Semiconductor from First-Principles. *Comput. Mater. Scienc.* **2008**, *43*, 392−398.
(11) Theodoropolpu, N.; Hebard, A. F.; Overberg, M. E.; Abernathy, C. R.; Pearton, S. J.; Chu, S. N.; Wilson, R. G. Magnetic and Structural Properties of Mn-Implanted GaN. *Appl. Phys. Lett.* **2001**, *78*, 3475−3477.
(12) Foutz, B. E.; O'Leary, S. K.; Shur, M. S.; Eastman, L. F. Transient Electron Transport in Wurtzite GaN, InN, and AlN. *J. Appl. Phys.* **1999**, *85*, 7727−7734.
(13) Zubrilov, A. *Properties of Advanced Semiconductor Materials GaN, AlN, InN, BN, SiC, SiGe*; Levinshtein, M. E.; Rumyantsev, S. L.; Shur, M. S., Eds.; Wiley: New York, 2001; Chapter 2, pp 49−50.
(14) Davydov, V.Yu.; Klochikhin, A. A.; Emtsev, V. V.; Smirnov, A. N.; Goncharuk, I. N.; Sakharov, A. V.; Kurdykov, D. A.; Baidakova, M. V.; Vekshin, V. A.; Ivanov, S.; et al. Photoluminescence and Raman Study of Hexagonal InN and In-rich InGaN Alloys. *Phys. Status Solidi B* **2003**, *240*, 425−428.
(15) Ney, A.; Rajaram, R.; Farrow, R. F. C.; Harris, J. S.; Parkin, S. P., Jr. A Promising Diluted Magnetic Semiconductor Material. *J. Supercond: Novel Magnet.* **2005**, *18*, 41−46.
(16) Gan, C. K.; Srolovitz, D. J. First-Principles Study of Wurtzite InN (0001) and (000$\bar{1}$) Surfaces. *Phys. Rev. B* **2006**, *74*, 115319−115324.
(17) Segev, D.; Van de Walle, C. G. Surface Reconstructions on InN and GaN Polar and Nonpolar Surfaces. *Surf. Sci.* **2007**, *601*, L15−18.
(18) Song, J. H.; Akiyama, T.; Freeman, A. J. Stabilization of Bulk p-Type and Surface n-Type Carriers in Mg-Doped InN {0001} Films. *Phys. Rev. Lett.* **2008**, *101*, 186801−185805.
(19) Belabbes, A.; Kioseoglou, J.; Komninou, Ph.; Evangelakis, G. A.; Ferhat, M.; Karakostas, Th. Magnesium Adsorption and Incorporation in InN (0 0 0 1) and Surfaces: A First-Principles Study. *Appl. Surf. Sci.* **2009**, *255*, 8475−8482.
(20) Jaffe, J. E.; Snyder, J. A.; Lin, Z.; Hess, A. C. LDA and GGA Calculations for High-Pressure Phase Transitions in ZnO and MgO. *Phys. Rev. B* **2000**, *62*, 1660−1665.
(21) Vanderbilt, D. Soft Self-Consistent Pseudopotentials in Generalized Eigenvalue Formalism. *Phys. Rev. B* **1990**, *41*, 7892−7895.
(22) Rinke, P.; Winkelnkemper, M.; Qteish, A.; Bimberg, D.; Neugebauer, J.; Scheffler, M. Consistent Set of Band Parameters for the Group-III Nitrides AlN, GaN, and InN. *Phys. Rev. B* **2008**, *77* (075202), 1−15.
(23) Miyajima, T.; Kudo, Y.; Liu, K. L.; Uruga, T.; Honma, T.; Saito, Y.; Hori, M.; Nanishi, Y.; Kobayashi, T.; Hirata, S. Structure Analysis of InN Film Using Extended X-ray Absorption Fine Structure Method. *Phys. Status Solidi B* **2002**, *234*, 801−804.
(24) Davydov, V. Yu.; Klochikhin, A. A.; Seisyan, R. P.; Emtsev, V. V.; Ivanov, S. V.; Bechstedt, F.; Furthmuller, J.; Harima, H.; Mudryi, A. V.; Aderhold, J.; et al. Absorption and Emission of Hexagonal InN: Evidence of Narrow Fundamental Band Gap. *Phys. Status Solidi B* **2002**, *229*, r1−r3.
(25) Sato, K.; Dederichs, P. H.; Katayama-Yoshida, H.; Kudrnovsky, J. Exchange Interactions in Diluted Magnetic Semiconductors. *J. Phys.: Condens. Matter* **2004**, *16*, S5491−S5497.